

Metal Chelates of Azo-Pyridazine Dyes III Chelating Tendencies of Pyruvic and Hippuric Monohydrzone-3-hydrazino-4-benzyl-6-phenylpyridazine

Atef A. T. Ramadan^a, Magdy H. Seada^a, and Emil N. Rizkalla^{b,*}

^a Faculty of Education, Ain Shams University, Roxy, Cairo, Egypt

^b Faculty of Science, Ain Shams University, Abbassia, Cairo, Egypt

(Received 2 April 1984. Accepted 14 May 1984)

The synthesis and quantitative equilibrium studies of two new azo-pyridazine ligands, namely the pyruvic (*PHP*) and hippuric (*HipHP*) acid derivatives are described in detail. Their acid-base and metal-ligand equilibrium constants in 75% dioxan-water solvent at 30 °C have been calculated from potentiometric and spectrophotometric data. The probable structures are inferred from electronic and vibrational spectral results. Evidence is presented for the formation of protonated complexes with *PHP*.

(Keywords: Azo-pyridazine dyes; Lanthanide ions; Stability constants; Transition metals)

Metall-Chelate von Azo-pyridazin-Farbstoffen, 3. Mitt.: Chelationsvermögen von Monohydrzon-3-hydrazino-4-benzyl-6-phenylpyridazin-Derivaten der Brenztrauben- und Hippursäure

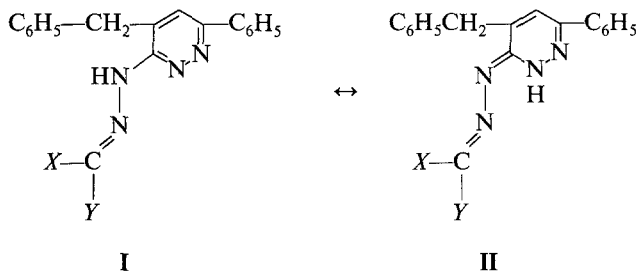
Die Synthese und quantitative Gleichgewichtsuntersuchungen von zwei neuen Azo-pyridazin-Liganden, die von Brenztraubensäure (*PHP*) bzw. Hippursäure (*HipHP*) abzuleiten sind, werden im Detail beschrieben. Die entsprechenden Säure-Base- und Metall-Ligand-Gleichgewichtskonstanten in 75% Dioxan-Wasser bei 30 °C wurden aus potentiometrischen und spektrophotometrischen Daten ermittelt. Die wahrscheinlichen Strukturen wurden von Elektronen- und IR-spektroskopischen Daten abgeleitet. Es sind Beweise vorhanden, daß mit *PHP* protonierte Komplexe gebildet werden.

Introduction

The versatility of ligand dyes as analytical reagents has resulted in a considerable interest in connection with the synthesis of new and structurally related compounds. Also, a substantial significance has been

attached to comparisons between the chelating abilities of these species with a particular transition metal ion and its dyeing properties. The implications of such structural variations on the absorption characteristics of the azo-dye chelates have been discussed thoroughly by *Yagi*¹. Based on his results, it was possible to conclude that the extent of the $d\pi-p\pi$ interaction between the hydrazone group and the central metal ion is determined by the type and position of the different substituents relative to the chromophoric system. Strong acidic groups such as sulphonic acid groups are believed to act only as solubilizing centers² particularly if they are stereochemically unavailable to coordinate the $(N=N) \rightarrow M$ center. Their influence on coordination will be limited to electrometric effects. Strong donating *ortho* substituted derivatives are, on the other hand, recognized to have superior dyeing properties and are expected to develop progressively.

In previous papers^{3,4} the chelating ability of a series of substituted 3-hydrazino-4-benzyl-6-phenylpyridazine ligands (structures I and II) have been studied with transition and lanthanide metal ions.



<i>BEHP</i>	$(X = C_2H_5-; Y = C_6H_5-)$
<i>BAHP</i>	$(X = CH_3-; Y = -CH=C(OH)-C_6H_5)$
<i>DAHP</i>	$(X = CH_3-; Y = -CO-CH_3)$
<i>BHP</i>	$(X = C_6H_5-; Y = -CO-C_6H_5)$
<i>PHP</i>	$(X = CH_3-; Y = -COOH)$
<i>HipHP</i>	$(X = C_6H_5-; Y = -NH-CH_2-COOH)$

The results indicate that the parent compound *BEHP* (both *X* and *Y* are hydrocarbons) behaves as a bidentate ligand using the pyridazine ring nitrogen and the azo nitrogen farthest from the nucleus. The introduction of an enolic hydroxy group alters the mode of coordination thus freezing the pyridazine nucleus in a *trans* position to the coordination center as indicated by spectroscopic and equilibrium data for the *BHP* and *DAHP*

systems⁴. In the case of *BAHP*, the free rotation around the C—C single bond of the aliphatic chain allows a concurrent coordination of the three donor sites in the dye molecule. In all cases, the ligands behave as monoprotic species except under drastic conditions of reflux with copper salts, where two gram equivalents of hydrogens are lost—probably those of the hydrazo and enolic groups.

In order to obtain additional information on the relation between dye structure and chelation, the metal stability constants and spectral characteristics of the structurally related condensation products of pyruvic (*PHP*) and hippuric (*HipHP*) acids with 3-hydrazino-4-benzyl-6-phenylpyridazine have been studied. The structures of these chelating agents differ from that of the parent ligand, in that in the first a carboxylic group substitutes the phenyl nucleus in the *Y* position and in the second the *Y* group is replaced by a glycinate arm. In both cases, the chromophoric system is retained.

Experimental

Preparation of the Solid Ligands

PHP was obtained by mixing a freshly prepared ethanolic solution of 3-hydrazino-4-benzyl-6-phenylpyridazine⁵ with an equivalent amount of pyruvic acid. The mixture was stirred at room temperature where a pale yellow liquid resulted. This was left in a refrigerator for 24 h where a yellow solid is obtained. The product was recrystallized from ethanol to give yellow crystals, m.p. 136°; yield = 80%. Anal. Calcd. for $C_{20}H_{18}O_2N_4 \cdot H_2O$: C 65.93, H 5.49, N 15.38. Found: C 65.86, H 5.38, N 15.32.

HipHP was prepared by refluxing an ethanolic solution of the hydrazino-pyridazine derivative with the stoichiometric amount of hippuric acid for 2 h. The solid separated upon cooling was filtered, washed and recrystallized from ethanol as brown crystals. Yield = 60%. Anal. Calcd. for $C_{26}H_{23}O_2N_5$: C 71.40, H 5.26, N 16.02. Found: C 71.32, H 5.21, N 15.90.

*Preparation of the Cu-*PHP* Complex*

The solid copper complex was prepared by refluxing equimolar quantities of *PHP* and copper nitrate in aqueous dioxan for 20 min. Greenish crystals separated gradually. These were filtered, washed several times with aqueous dioxan and dried to a constant weight under vacuum. Anal. Calcd. for $Cu(HL)(NO_3) \cdot H_2O$: C 49.23, H 3.90, N 14.36, Cu 13.03. Found: C 49.11, H 3.95, N 14.29, Cu 13.01.

Reagents

All reagents were of analytical-reagent grade. Rare earth oxides of 99.9% purity (B.D.H.) were dissolved in nitric acid, the excess acid was removed by evaporation, and the concentrations of the $Ln(NO_3)_3$ were determined complexometrically with *EDTA* using hexamine buffer and xylenol orange serves as an indicator⁶. Other metal ion solutions were prepared from the corresponding

nitrate salts and standardized by conventional methods⁶. Dioxan was purified and distilled prior to each use as described elsewhere³. The base used was carbonate-free KOH kept under nitrogen atmosphere and standardized against primary standard potassium-hydrogenphthalate.

Measurements

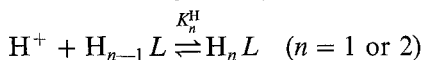
The potentiometric titrations were carried out using a Beckman SSR 2 *pH*-meter fitted with a combined glass-calomel electrode. In each run, 30 ml aliquots of the metal ligand mixture in 75% dioxan-water solvent were titrated with standard base (0.10 *M*). The correction for the measured *pH* values was taken as 0.28 units⁷. Solutions were adjusted to 0.10 *M* ionic strength by the addition of KNO₃ and maintained at 30 °C with constant-temperature water circulated through a sealed jacketed cell. Purified nitrogen gas was passed through the solution during the measurements.

The visible-UV absorptions of the ligands and their metal chelates were measured on a Prolabo UV-visible spectrophotometer using 1 cm matched cells and thermostated at 25 °C. Infrared spectra were obtained as KBr discs using a Pye Unicam SP 200 spectrophotometer.

Results

Ligand Protonation Constants

The potentiometric titration curves of *PHP* and *HipHP* are shown in Figs. 1 and 2 respectively. One proton dissociates between $a = 0$ and $a = 1$ (where a is the moles of base added per mole of ligand present). At higher *pH* values, one additional proton dissociates as indicated by the metal-ligand titration curves. For the general protonation equilibrium:



the constants, K_n^{H} were determined from the hydrogen ion concentrations of the ligand solution for each increment of the base added. The values of these constants were calculated using the general relationship:

$$\log K_n^{\text{H}} = \log \frac{(1-a+m-n)C_L - [\text{H}^+] + [\text{OH}^-]}{(a-m+n)C_L + [\text{H}^+] - [\text{OH}^-]} + pH \quad (1)$$

where m is the ligand basicity. The value of the ionic product, pK_w , of water in 75% dioxan-water medium was taken as 18.7⁸. The results obtained are given in Table 1. For comparison the protonation constants for the closely related ligands *BEHP*, *DAHP*, *BHP*, and *BAHP* are also listed.

PHP-Metal Ion Interactions

The *PHP* curves obtained with 2 : 1 molar ratios of ligand to Mn(II), Co(II), Ni(II), Cu(II), Zn(II) and Cd(II) ions are shown in Fig. 1. Similar

Table 1. Protonation constants of azo-pyridazine dyes^a

Ligand ^b	$\log K_1^H$	$\log K_2^H$
<i>PHP</i>	11.75 ± 0.03	6.40 ± 0.01
<i>HipHP</i>	13.37 ± 0.04	6.51 ± 0.01
<i>BEHP</i>	13.75	
<i>DAHP</i>	12.94	
<i>BHP</i>	13.72	
<i>BAHP</i>	11.98	

^a All values determined at 30 °C; $\mu = 0.10 M$ (KNO_3) and in 75% dioxan-water solvent.

^b Ligands abbreviation are defined in the text.

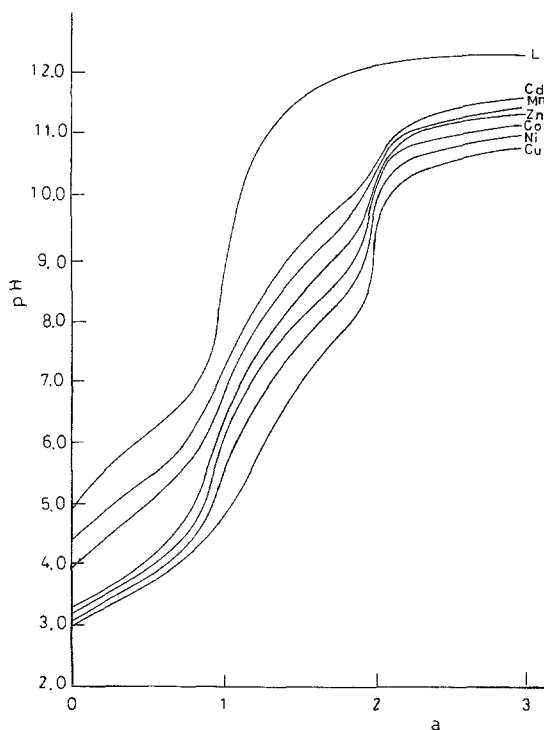


Fig. 1. Potentiometric equilibrium curves for 1 : 2 molar ratios of metal ions to *PHP* in 75% dioxan-water solvent; $a =$ moles of base added per mole of ligand; concentration is 0.001 M in metal ion, solution contains 0.10 M KNO_3 , $t = 30$ °C

Table 2. Equilibrium constants for the interaction of PHP with metal ions^a

A. Transition Metal Ions

Symbol	Equilibrium quotient	Mn ²⁺	Co ²⁺	Ni ²⁺	Log (Equil. Const.) Cu ²⁺	Zn ²⁺	Cd ²⁺	Fe ³⁺	UO ₂ ²⁺
$K_{M(HL)}^M$	$\frac{[M(HL)]^{(\xi-1)+}}{[M^{z+}][HL^-]}$	4.16 (± 0.03)	4.74	5.30	5.42	4.92	3.60	6.05	5.54
$K_{M(HL)_2}^M$	$\frac{[M(HL)_2^{(\xi-2)+}]}{[M^{z+}][HL^-]^2}$	8.21 (± 0.07)	10.55	10.80	11.14	10.30	7.14	12.06	10.58
$K_{ML(HL)}^M$	$\frac{[ML(HL)]^{(\xi-3)+}}{[M^{z+}][L^{2-}][HL^-]}$	11.44 (± 0.10)	14.58	15.82	16.45	14.06	9.81	18.77	15.50
$K_{ML_2}^M$	$\frac{[ML_2^{(\xi-4)+}]}{[M^{z+}][L^{2-}]^2}$	13.61 (± 0.10)	17.59	18.70	20.28	16.54	11.66	24.51	18.52
$K_{M(HL)_2}^H$	$\frac{[M(HL)_2^{(\xi-2)+}]}{[ML(HL)]^{(\xi-3)+}[H^+]}$	8.52 (± 0.05)	7.72	6.73	6.44	7.99	9.08	5.04	6.83
$K_{ML(HL)}^H$	$\frac{[ML(HL)]^{(\xi-3)+}}{[ML_2^{(\xi-4)+}][H^+]}$	9.58 (± 0.05)	8.74	8.87	7.92	9.27	9.90	6.01	8.73

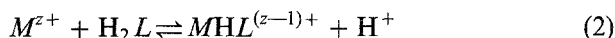
Table 2 (continued)

B. Lanthanide Ions

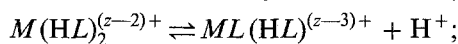
Cation	$\log K_{M(HL)}^M$	$\log K_{M(HL)_2}^M$
La ³⁺	4.50 (± 0.05)	9.68 (± 0.10)
Pr ³⁺	4.78	10.35
Nd ³⁺	4.96	10.68
Sm ³⁺	5.30	10.80
Eu ³⁺	5.49	10.91
Gd ³⁺	5.45	11.05
Tb ³⁺	5.32	10.97
Dy ³⁺	5.33	11.18
Ho ³⁺	5.26	10.72
Er ³⁺	5.37	10.70
Tm ³⁺	5.32	10.84
Yb ³⁺	5.35	10.75
Lu ³⁺	5.39	10.69

^a $\mu = 0.10 M$ (KNO₃), 30 °C in 75% dioxan-water medium.

plots are obtained in the case of Fe(III) and UO₂²⁺ systems. With trivalent lanthanide ions, slight hydrolysis was observed beyond the completion of the buffer region between $a = 1$ and $a = 2$. The shapes of these curves clearly indicate the formation of simple mononuclear chelates as well as various protonated species. The complex equilibria in the first buffer region may be represented by:

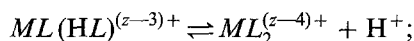


Further addition of base results in the subsequent dissociation of two protons as indicated by the amount of base required per metal chelate. The reactions involved may be described by the equilibria:



$$K_{M(HL)_2}^H = [M(HL)_2^{(z-2)+}] / [ML(HL)^{(z-3)+}] [H^+] \quad (4)$$

and

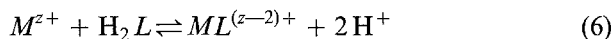


$$K_{ML(HL)}^H = [ML(HL)^{(z-3)+}] / [ML_2^{(z-4)+}] [H^+] \quad (5)$$

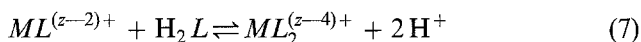
Computer assisted algebraic methods were used to solve for the two overlapping complex protonation constants involved in the second buffer region. The results obtained together with the corresponding formation constants of $M(HL)^{(z-1)+}$ and $M(HL)_2^{(z-2)+}$ species are summarized in Table 2.

HipHP-Metal Ion Interactions

The potentiometric titration curves of the *HipHP* complexes of transition metal ions are very similar, as is indicated in Fig. 2. However, they differ from *PHP* curves in that the former shows the presence of only one long buffer region from $a = 0$ to $a = 2$. The constants for the overlapping equilibria:



and



were calculated from the expressions of equilibrium constants for eqs. (6) and (7), and the mass balance and charge balance equations⁹. All the stability constants are listed in Table 3.

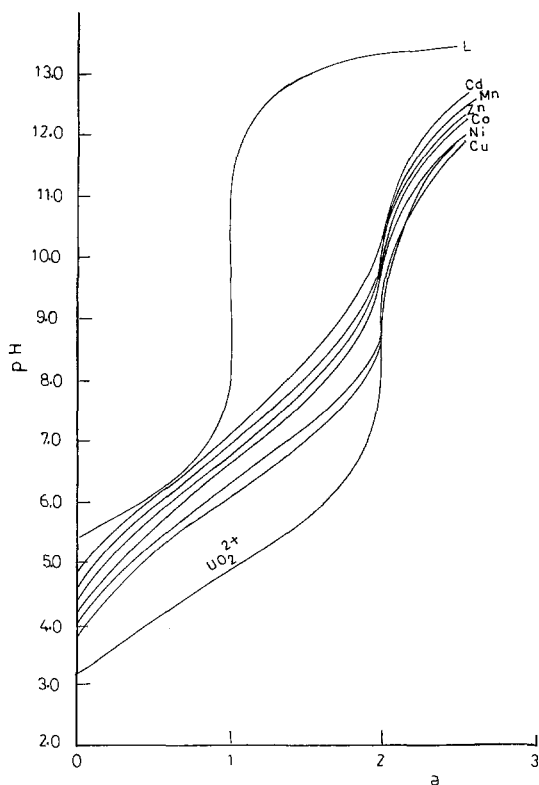


Fig. 2. Potentiometric titration curves for 1 : 2 molar ratios of metal ions to *HipHP* in 75% dioxan-water solvent; a = moles of base added per mole of ligand; concentration is 0.001 M in metal ion, solution contains 0.10 M KNO_3 , $t = 30^\circ C$

Table 3. *Equilibrium constants for the interaction of HipHP with metal ions*^a

A. Divalent Metal Ions			
Metal Ion	Potentiometric Results		Spectrophotometric Results $\log K_{ML}^M$ ^d
	$\log K_{ML}^M$ ^b	$\log K_{ML_2}^M$ ^c	
Mn ²⁺	9.19	16.97	
Co ²⁺	9.96	18.14	10.12
Ni ²⁺	11.05	19.84	10.89
Cu ²⁺	11.81	20.88	11.85
Zn ²⁺	9.64	17.69	
Cd ²⁺	8.79	16.27	
UO ₂ ²⁺	14.42	25.80	

B. Lanthanide Ions		
Cation	$\log K_{ML}^M$	$\log K_{ML_2}^M$ ^c
La ³⁺	10.97 (± 0.05)	21.19 (± 0.10)
Ce ³⁺	11.08	21.47
Pr ³⁺	11.25	21.72
Nd ³⁺	11.42	22.05
Sm ³⁺	11.72	22.41
Eu ³⁺	11.87	22.66
Gd ³⁺	12.03	22.54
Tb ³⁺	11.87	22.28
Dy ³⁺	11.81	21.95
Ho ³⁺	11.65	22.09
Er ³⁺	11.61	22.15
Tm ³⁺	11.70	22.28
Yb ³⁺	11.75	22.23
Lu ³⁺	11.76	22.29

^a All measurements at $\mu = 0.10$ M (KNO₃), 30 °C and in 75% dioxan-water solvent.

^b (± 0.03).

^c (± 0.08).

^d (± 0.10).

^e The equilibrium constants $K_{ML_2}^M$ were calculated in the region between $\alpha = 0.5$ and $\alpha = 1.5$ because of the uncertainties in pH measurements beyond this region as a result of metal hydrolysis.

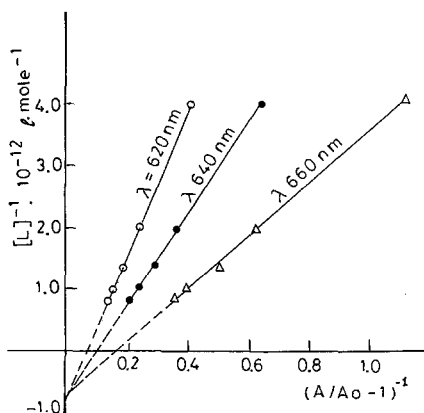


Fig. 3. *Nach's* plots of $[L]^{-1}$ vs. $(A/A_0 - 1)^{-1}$ for the Cu—*HipHP* system in 75% dioxan-water solvent. A and A_0 are the absorbances in the presence and absence of ligand; $\mu = 0.10 M$ KNO_3 , $t = 25^\circ C$

Since copper, nickel, and cobalt chelates have intense colors and absorb in the region 500–600 nm, the formation constants of these species have been further assessed spectrophotometrically. In the region of overlapping spectrograms of the free metal ion and its complex, and assuming that only 1:1 complexes are formed ($C_L/C_M < 0.3$), the following relationship holds¹⁰:

$$[L^{2-}]^{-1} = (1 - A/A_0)^{-1} (K_{ML}^M - \alpha) - K_{ML}^M \quad (8)$$

where A and A_0 are the absorbances in the presence and in the absence of *HipHP*, $\alpha = K_{ML}^M \epsilon_c / \epsilon_m$ and ϵ_c and ϵ_m are the molar extinctions of the complex and the metal ion respectively. Plots of $[L^{2-}]^{-1}$ vs. $(1 - A/A_0)^{-1}$ gives a straight line whose intercept is K_{ML}^M . The free ligand concentration has been calculated at any particular pH using the equation:

$$C_L = [L^{2-}] \{1 + K_1^H [H^+] + K_1^H K_2^H [H^+]^2\} \quad (9)$$

A sample set of these calculations is presented in Fig. 3, and the results obtained are included in Table 3 (A).

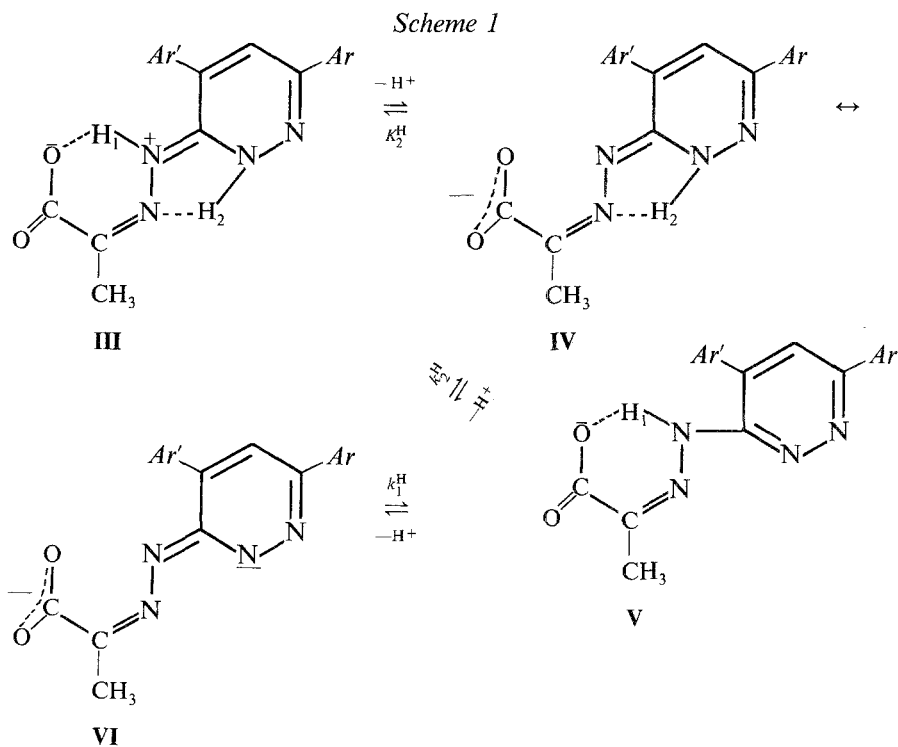
Discussion

Ligand Protonation Constants

The values of the two protonation constants of *HipHP* listed in Table 1 are consistent with the structure of this ligand. If the *HipHP* molecule is considered to consist of a 3-hydrazino-pyridazine group condensed with a hippuric acid molecule, then the first protonation constant is associated with the highly basic pyridazine nitrogen and probably hydrogen-bonded to the hydrazo nitrogen farthest from the ring. This is evident from the

close resemblance of K_1^H values for this ligand and for the parent *BEHP* molecule. Addition of a second proton binds the glycine part of the hippurate arm. Obviously, pK_2^H is much lower than that of glycine (9.60 at $\mu = 0,1$; aqueous¹¹), since in the former case protonation takes place on a secondary nitrogen which is deshielded by the inductive effect of the adjacent azomethine group. A similar trend in pK_1^H values has been observed for the closely related substances glutamic and benzoylglutamic acids ($pK_1^H = 9.46$ and 4.63 respectively at $\mu = 0,1$; aqueous¹²). The drop of 4.8 log units compares well with the difference $\Delta [pK_2^H(\textit{HipHP}) - pK_1^H(\textit{glycine})]$ if an allowance is made for the differences in the medium and the electron withdrawing effects of $>C=O$ and $>C=N$ groups.

The protonation constants of *PHP* can be best understood through a comparison with other related ligands. As is seen from the data in Table 1, pK_1^H value for *PHP* is approx. 2 log units lower than those estimated for *BEHP*, *BHP*, and *DAHP*. It is also of interest to note that the pK_2^H value is 4 log units higher than that of pyruvic acid¹³ and $\approx 3-4$ log units higher than that of typical α -substituted acids¹⁴. Such differences cannot be correlated with simple electrometric or solvent effects and are perhaps due to a major tautomeric rearrangement as indicated in Scheme 1.



This explains the similarity of K_2^H values for both *PHP* and *HipHP* species. Also, the apparent K_1^H value obtained for the *PHP* ligand is in fact an average for the intrinsic basicities of the pyridazine (ca. 13.7) and azo (ca. 9) group nitrogens (tautomers **IV** and **V**) as determined by the microscopic constants k_1^H and k_2^H .

Complexation Studies

The trivalent lanthanide ions, all having the same outer electronic configuration, form a unique series for a study of the influence of the size of the central ion on the coordination properties of various ligands. For a purely electrostatic interaction, the strength of the bond is expected to increase linearly with increasing the ionic potential Z^2/r where Z is the cationic charge and r is the ionic radius. This behavior holds for the La—Eu chelates as is seen in Fig. 4. Beyond Dy—Ho, the change in β value is very small. The complex nature of the region Gd—Dy is associated with changes in solvation properties of the cations^{15,16}.

The active segment of these chelating agents responsible for the lanthanide ion coordination is the hydrazo-carboxylate arm in the case of

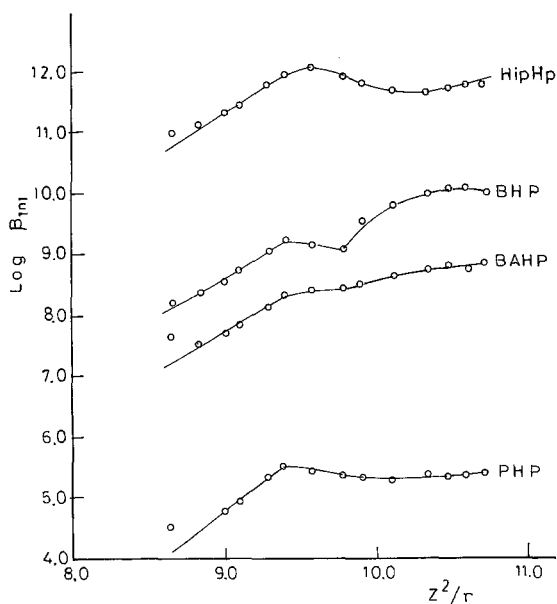


Fig. 4. Plots of $\log \beta_{1n1}$ for the various lanthanide-azo pyridazine chelates as a function of the ionic potential Z^2/r . $n = 0$ in the case of *HipHP*, *BHP*, and *BAHP* and $n = 1$ for *PHP*

PHP and *HipHP* or the hydrazo-ketonic segment as is the case of *BAHP* and *BHP*. However, all are similar in that they behave as N,O donors toward the rare earth ions forming either 5- or 6-membered chelate rings. Accordingly, a plot of $\log \beta_{101}$ ($\log \beta_{111}$ in the case of *PHP*) as a function of the respective ligand basicity (i.e., $\sum pK_i^H$) is expected to be a straight line of unit slope¹⁷. The deviation from unit slope, i.e., $\log \beta$ values are always smaller than predicted (cf. Fig. 5) is perhaps associated with significant steric effects of the substituent adjacent to the chelating centers. The steric arguments are consistent with the monotonous increase in β values of the *BHP* chelates with decreasing r . The rigid structure of the molecule strengthens the metal-nitrogen interaction. On the other hand, molecules of greater rotational freedom such as *HipHP* and *PHP* display maxima at $r_+ \simeq 0.94 \text{ \AA}$.

An attempt to rationalize the trend of β values for a particular transition metal with the various chelating dyes in terms of the ligands basicity is unsuccessful. This discrepancy is partly ascribed to the failure of the measured pK_i^H values to account for the intrinsic basicity of the ligand molecules felt by the metal ion. The basicity of other coordination active centers are not included in the $\sum pK$ term.

The structure of *HipHP* allows a reasonable arrangement of three coordinate bonds around the metal ion as indicated by the formula VII (Scheme 2).

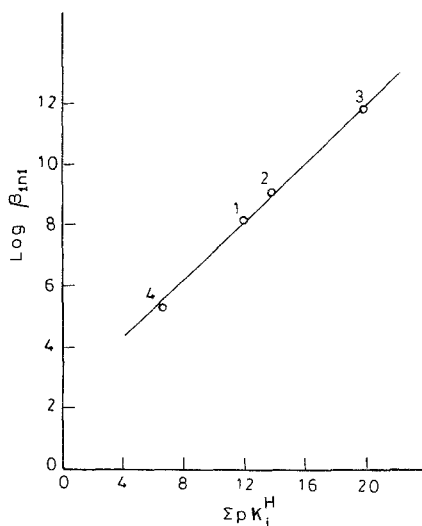
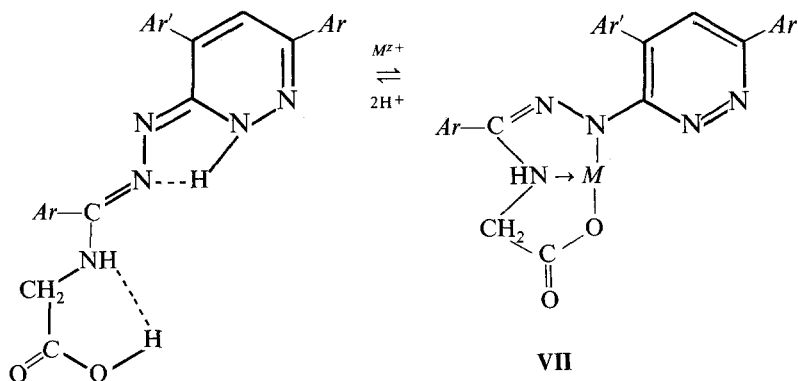


Fig. 5. Relationship between the values of $\log \beta_{1,n1}$ for the formation of SmH_nL and $\sum pK_i^H$. $n = 0$ for *BAHP* (1), *BHP* (2), and *HipHP* (3) and $n = 1$ for *PHP* (4)

Scheme 2



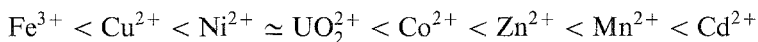
The extensive changes in the absorption spectra of the free ligand upon coordination with metal ions (cf. Table 4) supports the conclusion implied in the above discussion. The appearance of a new band in the region 350–370 nm is probably associated with the formation of metal-hydrazoate linkages and may be caused by a $\pi \rightarrow d$ charge transfer process. The tailing off of this new band in the visible region masks the weak $d \rightarrow \pi$ transitions for the nickel and copper species whereas that of cobalt is displayed at 438 nm.

PHP forms stable *MHL* chelates as evidenced both by the inflection at $a = 1$ in the titration curves and the isolation of the solid copper species. The structure of these species can be inferred from the changes in the IR absorption bands of the free ligand and its copper chelate. The shift in the $\nu_{C=O}$ band of the carboxylate group from 1700 cm^{-1} to 1670 cm^{-1} and the appearance of a strong band at 625 cm^{-1} assigned to the ν_{M-O} bond is indicative of a carboxylate coordination to the metal ion. Probable arrangement of the donor groups is shown in **III** with *M* replacing H_1 . As

Table 4. *UV Spectral characteristics of HipHP and its metal chelates*

Species	λ_{\max}/nm	$\log \epsilon_{\max}$
H_2L	270	4.16
CoL	385	3.04
	355	3.46
NiL	438	3.10
	352	3.32
CuL	370	2.95

more base is added, the *pH* becomes sufficiently high to assist in the dissociation of the protons attached to the pyridazine group. The basicity of this proton is not as strong as in the free ligand and is influenced appreciably by the present metal ion, following the order:



which is the reversed order for the stabilities of the normal chelates. The deprotonation process is accompanied by a structural rearrangement to allow for the simultaneous coordination of the pyridazine nitrogen.

The variation of $\Delta \log \beta_{102}$, the increment of stability of the *HipHP* over the *PHP* chelate, is seen to be roughly a measure of the importance of steric factors in grouping the six donor sites (4 in the case of Cu-chelates) around the metal ions. Metal ions of favorable coordination number 4 have comparable affinities towards *PHP* and *HipHP*. Large cations such as UO_2^{2+} and Cd^{2+} can afford sterically the accommodation of the six donor sites of the *HipHP* molecules where with *PHP* the simultaneous participation of both pyridazine nuclei in the coordination sphere is not favorable.

References

- ¹ Yagi Y., Bull. Chem. Soc. Japan **36**, 487; 492; 500; 506; 512 (1963).
- ² Snavely F. A., Sweigart D. A., Inorg. Chem. **8**, 1659 (1969).
- ³ Ramadan A. A. T., Seada M. H., Rizkalla E. N., Talanta **30**, 245 (1983).
- ⁴ Rizkalla E. N., Ramadan A. A. T., Seada M. H., Polyhedron **2**, 1155 (1983).
- ⁵ Jahine H., Zaher H. A., Sayed A., Seada M., Indian J. Chem. **15B**, 352 (1977).
- ⁶ West T. S., Complexometry with *EDTA* and Related Reagents. London: Broglia Press. 1969.
- ⁷ Irving H. M. N. H., Mahnot U. S., J. Inorg. Nucl. Chem. **30**, 1215 (1968).
- ⁸ Goldberg D. E., J. Chem. Education **40**, 341 (1963).
- ⁹ Incézdý J., Analytical Applications of Complex Equilibria. Chichester: Horwood. 1976.
- ¹⁰ Nach C. P., J. Phys. Chem. **64**, 950 (1960).
- ¹¹ Gregely A., Nagypal I., Mojzes J., Acta Chim. Acad. Sci. Hung. **51**, 381 (1967).
- ¹² Nyberg M. H. T., Cefola M., Sabine D., Arch. Biochem. Biophys. **85**, 82 (1959); Nyberg M. H. T., Cefola M., *ibid.* **111**, 321 (1965).
- ¹³ Leussing D. L., Hanna E. M., J. Amer. Chem. Soc. **88**, 693 (1966).
- ¹⁴ Sillén L. G., Martell A. E., Stability Constants of Metal-Ion Complexes, Spec. Publ. No. 25. London: The Chemical Society. 1971.
- ¹⁵ Grenthe I., Acta Chem. Scand. **18**, 293 (1964).
- ¹⁶ Degischer G., Choppin G. R., J. Inorg. Nucl. Chem., 1972, **34**, 2823.
- ¹⁷ Irving H., Rossotti H., Acta Chem. Scand. **10**, 72 (1956).